Controlling Protein Orientation in Vacuum Using Electric Fields

Erik G. Marklund,[*,†,‡] Tomas Ekeberg,[¶] Mathieu Moog,[§] Justin L.P. Benesch,[‡] and Carl Caleman[*,§,¶]

†*Department of Chemistry – BMC, Uppsala University, Box 576, SE-751 23 Uppsala, Sweden*

‡*Physical & Theoretical Chemistry Laboratory, Department of Chemistry, University of Oxford, South Parks Road, Oxford, GB-OX1 3QZ, United Kingdom*

¶*Center for Free-Electron Laser Research, Deutsches Elektronen Synchrotron, DE-22607, Hamburg, Germany*

§*Department of Physics and Astronomy, Uppsala University, Box 516, SE-751 20 Uppsala, Sweden*

E-mail: erik.marklund@kemi.uu.se; carl.caleman@physics.uu.se

Abstract

Single particle imaging using X-ray free-electron lasers is an emerging technique that could provide high-resolution structures of macromolecules in the gas phase. One of the largest difficulties in realising this goal is the unknown orientation of the individual sample molecules at the time of exposure. Pre-orientation of the molecules has been identified as a possible solution to this problem. Using molecular dynamics simulations, we identify a range of electric field strengths where proteins become oriented without losing their structure. For a number of experimentally relevant cases we show that structure determination is possible only when orientation information is included in the orientation-recovery process. We conclude that non-destructive field orientation of intact proteins is feasible and that it enables a range of new structural investigations with single particle imaging.

Graphical TOC Entry

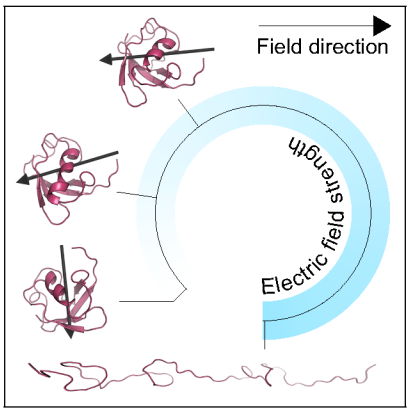

Traditional structural biology techniques require that all molecules are trapped in the same state, or alternatively they report ensemble averages that obscure the rich variety of molecular states in a sample.[1] Gas-phase approaches to structural biology can bypass some of these constraints, and inform about individual states and systems that are problematic for X-ray crystallography or NMR. For example, mass spectrometric techniques has provided much insight into the structure of macromolecules and their interactions and dynamics, but to a limited structural resolution.[2–4] Single particle imaging (SPI) is a set of emerging techniques that utilise ultra-short and ultra-intense X-ray pulses to generate diffraction from single isolated particles *in vacuo*.[5,6] Similar techiques using nanocrystals has exploited the small sample dimensions and short pulse durations to enable the study of systems and processes, such as short-lived intermediates, that are problematic for crystallography.[7–9] Non-crystalline targets present additional challenges, but can in principle be used in SPI to probe even more elusive structures.[5] Recently, this approach was used to image the Mimi virus, including its encapsulated genome.[10,11] Like in crystallography, SPI diffraction patterns collectively hold detailed 3D-information about the structure, but a fundamental and important difference lies in the sample handling. Instead of repeatedly exposing a single crystal to subsequent pulses from different angles, the sample particle is obliterated by the beam upon exposure in SPI, and each diffraction pattern comes from separate but identical particles. The pulses thus need to be sufficiently short and intense to generate diffraction before the structure is destroyed, which happens within tens of femtoseconds. This principle has become known as "diffraction before destruction".[12] Since the patterns each have unknown and random orientation in SPI [Fig. 1(a)], their assembly into a complete and self-consistent 3D dataset – a process known as 'orientation recovery' – is very challenging, requiring advanced algorithms that are not always able to arrive at the correct result.[13]

Expand, Maximize and Compress (EMC) is a state-of-the-art algorithm for this purpose.[14] It is an iterative algorithm where, for each pattern, EMC calculates the probability that it represents each of the sampled orientations given the 3D Fourier volume from the pre-

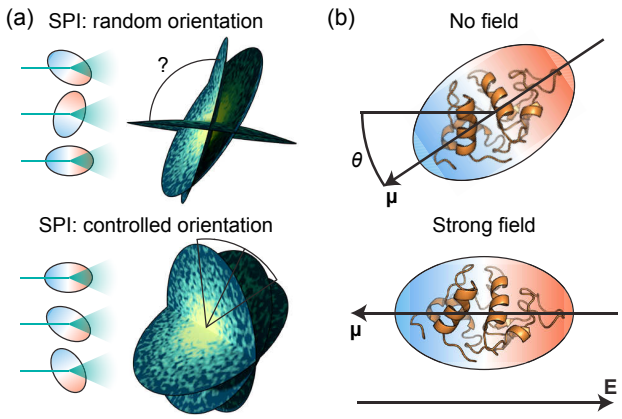

Figure 1: Orientation: weak and strong fields. (a) In SPI, controlled orientation could help relate individual diffraction patterns, facilitating the structure determination. (b) Dipolar molecules are randomly oriented in a weak electric field, but a strong field can in principle orient the dipole moment $\boldsymbol{\mu}$ along the field $\mathbf{E}$.

vious iteration. These probabilities are then used as weights when assembling the patterns into a new 3D Fourier volume. Incorporating additional information about the individual particles' orientation could be a means to reduce the complexity of this process, by reducing the ambiguity in the assembly process, enabling structure determinations that would otherwise be impossible. Controlling the particle's orientation is a potential strategy for obtaining such information. Indeed, controlled sample orientation, as illustrated in Fig. 1(a), has been recognised as a route in need of systematic investigation by the SPI community, and could be of utility for gas-phase biophysics and -chemistry more broadly.[13,15] The terms 'alignment' and 'orientation' both appear in the literature. They differ in that states that are antiparallel are considered equal in the former, but distinct in the latter. The idea of orienting or aligning molecules using external electric fields was introduced over two decades ago,[16] and alignment of small rather rigid molecules was also experimentally demonstrated around the same time.[17–19] Today alignment of small molecules in vacuum using laser fields is commonly practiced.[20–22] Alignment of small molecules has, for example, been shown to facilitate X-ray imaging of 2,5-diiodo-benzonitrile.[22] Controlled orientation or alignment could also be used to help distinguish between different conformations of macromolecules, which would be very valuable for structural biology.

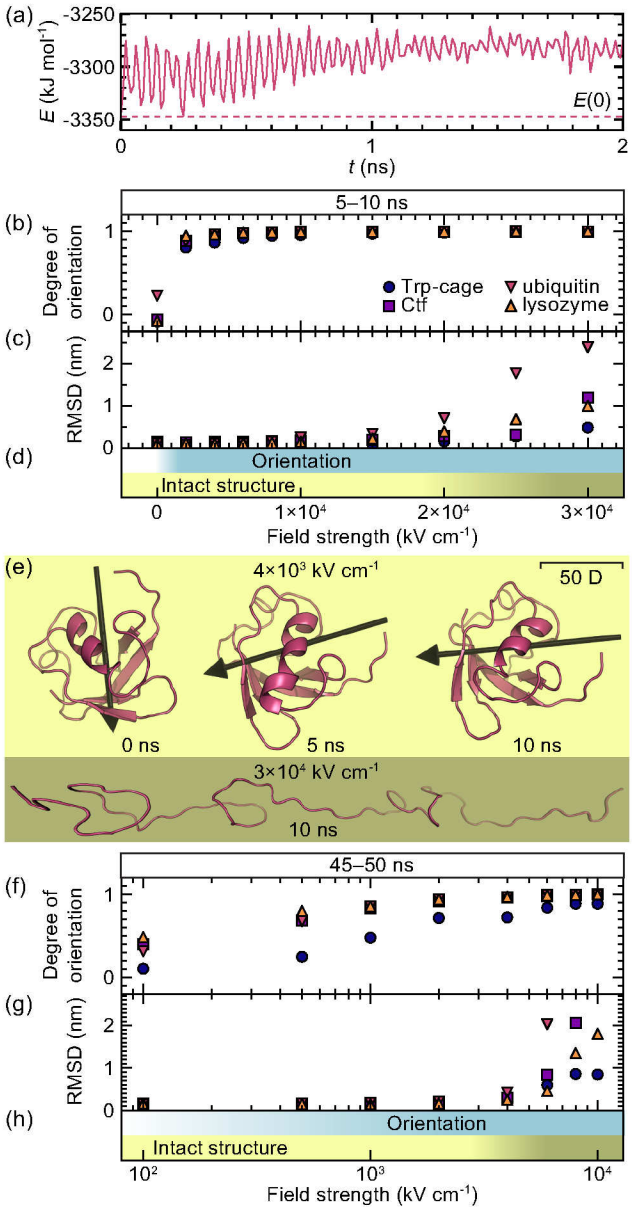

Figure 2: (a) The total internal energy – not including the dipole–field energy – during the first 2 ns of a ubquitin simulation with a 4000 kV cm^{-1} field. The dashed line shows the energy at $t = 0$. Fig. S3(a) is based on the same simulation. (b) The degree of orientation and (c) RMSD of the C_α over the last 5 ns of 10-ns simulations. (d) The regimes where orientation can be achieved and where nativelike structures are preserved on the 10 ns timescale. (e) Snapshots from a simulation of ubiquitin at 4000 kV cm^{-1} [same as in (a)], and one extreme case at 30 000 kV nm^{-1}. (f)–(h) Analogous to (b)–(d) for the 50-ns simulations (note the logarithmic x-axis). See Figs. S5–S10; Supplemental Videos 1 and 2.

Like small molecules, proteins often carry a net dipole.[23] In the presence of an external electric field, the interaction between the dipole and the field generates a torque that might be used for manipulating a protein's orientation, as illustrated in Fig. 1(b). The potential of the dipole–field-interaction is harmonic, and thus gives rise to pendular motions. These motions can be absorbed by a surrounding medium, such as a buffer gas, aligning the protein dipole with the field. This has been investigated in Ref.[23] Interaction with the gas lead to frictional forces however, causing substantial heating and unfolding.[24–26] In vacuum, the energy of the pendular motions cannot readily escape the protein. Under a rigid-body assumption the pendular motions are perpetual, but proteins are not rigid, and internal degrees of freedom can absorbe some of the pendular energy [Fig. 2(a)].[27] We hypothesise that for strong enough fields, this process can effectively orient a protein with the field direction. The question that follows is whether protein structures can withstand the strain and increased energy that the field interaction entails, or if they unfold before significant orientation takes place. Here, using molecular dynamics (MD) simulations, we first seek to test our hypothesis and see if orientation of native structures is possible. By developing and harnessing an augmented orientation-recovery algorithm, we then explore the potential benefit of controlled sample orientation for SPI.

To test our hypothesis, we conducted MD simulations of four small proteins [tryptophan cage (Trp-cage), the C-terminal fragment (Ctf) of the ribosomal protein L7/L12, ubiquitin and lysozyme; see Supporting Information, Figs. S1(a) and (b)] exposed to a range of fields, the latter being weak enough for ionisation to be unlikely.[28] The net charges of these proteins were all non-zero and in accordance with what can be observed with mass spectrometry. First, we inspected the total internal energy E (not including the field–dipole interaction) for any signs of absorption of pendular motions. We noted oscillations that decreased over time, accompanied by an overall energy increase. This observation, exemplified in Fig. 2(a), indicates that the pendular energy is indeed absorbed by the structure to some degree, corroborating our hypothesis.

Next, we asked if this repartitioning of energy is sufficient to cause significant orientation along the field direction. To answer this question, we monitored the degree of orientation, defined as $\cos(\theta)$, θ being the angle between the dipole moment and the field direction [Fig. 1(b)], over the last 5 ns of the 10-ns simulations. At all non-zero field strengths (2000–30 000 kV cm^{-1}), the proteins' orientations were close to unity [Figs. 2(b), S2 and S3(a)], and the timescale of orientation ranged from nanoseconds to tens of picoseconds [Fig. S3(b)]. Root mean square deviations (RMSDs) of the C_α atoms in the protein backbone above and below 0.5 nm indicate unfolded and structurally intact proteins, respectively (Supplemental Material).[29,30] Defining structural integrity according to this limit, we found that ubiquitin started to lose its structure at 20 000 kV cm^{-1}, and the other proteins did so at 25 000 kV cm^{-1} [Figs. 2(c), S4 and S5]. As these field strengths exceed those required for orientation, there is a "window" up to about $\leq$ 15 000 kV cm^{-1}, where dipole orientation of structurally intact proteins is feasible [Figs. 2(d) and (e), Supplemental Videos 1 and 2].

Since field orientation is not an instantaneous process, as illustrated by Figs. 2(a) and S3(a)–(b), the time a protein is exposed to the field might also be an important experimental parameter. To explore this further, we started a series of longer simulations (50 ns), where field strengths ranged down to 100 kV cm^{-1}. Here, the larger proteins oriented with the field to a large degree at 500 kV cm^{-1} and above, partially at 100 kV cm^{-1}, while remaining structurally intact up to about 4000 kV cm^{-1} [Figures 2(f)–(h), S6 and S7]. Comparing the results from the long simulations to the shorter simulations, we find that the position of the orientation window depends on the exposure time. Trp-cage was an exception to the trends seen in this second round of simulations, not being readily oriented in a nativelike state under these conditions, suggesting that dipole moment and mass might be important parameters too, and that orientation might be more feasible for high-mass proteins. This is promising for the analysis of larger proteins and complexes, which are more commonly the subject for structural biology. The gas-phase dipole moment of large proteins is currently largely unknown, and needs further investigation.

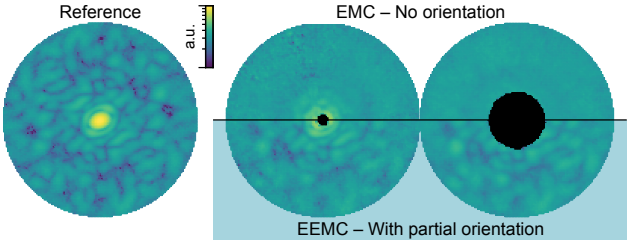

Figure 3: Utility for orientation recovery in SPI. The correct solution is shown to the left. Middle and right images show slices through the EMC (top) and EEMC (bottom) output. 3000 diffraction patterns and a 1.4 SP beam stop, and 10 000 patterns and a 5.6 SP beam stop, were respectively used for the middle and right images. Only EEMC converges in these cases. See also Figs. S2–S4.

We note that the timescales of our simulations was on par with the 10-ns high-field pulse length and 50-ns period of miniaturized ultra-FAIMS chips used for ion mobility spectrometry (albeit not in vacuum).[24] Such devices furthermore reach field strengths (75 kV cm^{-1}) that are comparable to the lower end of our range (100 kV cm^{-1}).[24,31] Even stronger fields are used for gas-phase separation of *ortho*- and *para*-forms of water, for manipulation of molecular beams, and for inducing dynamics in crystalline proteins.[32–34] These commensurate timescales and field strengths show that existing technology operates near a regime where our results indicate that field orientation of native protein structures can be achieved *in vacuo*. The boundaries of the orientation window depend on the exposure times, and native structures might be oriented under longer exposures at lower field strengths than those investigated here. This would be desirable, as fields approaching 1000 kV cm^{-1} are not readily produced in the laboratory, and may for other reasons be impractical for the application at hand.[33] To optimize the process of orientation and manipulation of proteins in vacuum, it is possible that a combination of static and oscillating fields is more suitable. This idea has been explored for small molecules, for example by Friedrich et al., but to the best of our knowledge no such studies focusing on proteins are available.[35,36] We have investigated proteins with a non-zero net charge, which would enable a range of manipulations in an experiment. While the acceleration of charged proteins has no impact on our results, the orientation timescales have practical consequences as they place geometric constraints on

any instrumentation, as the latter must accomodate the proteins' flight path sufficiently long for orientation to occur. The dislocation of small proteins, such as the ones studied herein, in static fields of 500 kV cm would be on the order of one or a few centimeters over 50 ns, which is still within laboratory length scales. For electrosprayed proteins, the net charge is determined by the surface area, whereas the mass scales with the volume.[37] The balancing of inertia and electrostatic force can thus be expected to yield shorter flight paths for larger proteins and complexes, which are normally of greater interest for structural biology.

Having established the feasibility of field orientation of native protein structures, we ask how useful it is for SPI. Here, in order to explore the value of field orientation in this context, we develop and benchmark an enhanced EMC (EEMC) that harness the 1D orientation information from field orientation of single proteins [Fig. S1(c)]. EMC searches for the optimal distribution of diffraction patterns in a given orientation space. In every iteration, each pattern is distributed over all iterations with a respective weight that corresponds to how well the pattern fits in that orientation given the previous iterate. This means that each pattern is not assigned a single orientation but many. Provided good signal strength and large enough number of patterns, this distribution over orientations will narrow to contain only the correct one.

In EEMC, we incorporate the information that we receive from field orientation as a prior used to modulate the distribution of each diffraction pattern. This will guide the algorithm to the correct orientation without enforcing it beyond the proper accuracy. In particular for the first iterations, where EMC often struggle to break the uniform distribution, this can significantly aid the algorithm. EEMC is in this way not restricted to field orientation but can utilize any prior information about the orientation. Notably, the orientation information is in this case not complete, as the orientation of the protein around the dipole axis remains unknown. Compounding this, the degree of orientation along the field may be off-unity, as shown in Fig. 2. These uncertainties have both been taken into account in our implementation.

Whenever EMC converged in our tests, EEMC did so between 25% and 50% faster (Fig. S8). We also find two situations where only EEMC converged to the correct solution (Fig. 3). I) when diffraction patterns are scarce: EMC only converged when having access to all 10 000 patterns, whereas EEMC converged with 3000 (Figure S9). This is reflected in the average angular error ϕ of the recovered orientations, which for 3000 patterns was 120.7° for EMC and 3.6° for EEMC. These numbers of images are on par with the 1000–20 000 useful diffraction patterns collected during 48-h beamtimes at the Linac Coherent Light Source. II) when the shadow of the beamstop, used to protect the center of the detector from the direct beam, is large: With 10 000 diffraction patterns, EMC converged for beamstop diameters up to 4.2 Shannon pixels (SP), whereas EEMC always found the correct solutions (Fig. S10). ϕ, for the largest tested beamstop, was 124.0° for EMC and 3.5° for EEMC.

The fact that the EEMC algorithm can utilise this type of incomplete orientational information is very promising and potentially makes it more robust when faced with challenges not investigated here, such as background noise or sample heterogeneity. Beamtime is currently very scarce. Being able to do successful reconstructions from a limited data volume is thus an important result from this work. Our findings could also have implications for other applications. For example, it was suggested that field orientation could prove useful for ion mobility spectrometry, giving access to information about the structural anisotropy, unreachable with the weak fields commonly used today.[23] Interactions with the buffer gas at high fields precludes orientation of native structures under the current principles for ion mobility spectrometry, but we hope that our study can inspire development of new concepts and technology to make orientation in high fields possible also in the presence of a buffer gas. We also imagine that field orientation can provide information about the dipole moments of proteins, hence their internal charge distributions, which is pertinent for native mass spectrometry.[38]

Using MD we demonstrated the possibility of orienting protein molecules *in vacuo* using static electric fields. We found a window where this is achieved in a nondestructive manner.

The bounds of this window depend on the time a protein is exposed to the field, and non-destructive orientation is achieved at, or near, timescales and fields strengths where existing technology operates. We showed that orientation of native protein structures makes a large impact for SPI. Besides this specific application, these findings can be transformative for gas-phase methods for protein chemistry and biophysics more broadly.

Computational Methods

Gas-phase structures and molecular topologies for Trp-cage, Ctf, ubiquitin, and lysozyme were taken from earlier MD simulations.[30] These were simulated with GROMACS for 10 or 50 ns in electric fields ranging from 0 to 30 000 kV cm^{-1}.[39] Each combination of protein and field strength was simulated 10 times with different random starting orientations. See Supporting Information for a full description of the MD simulations.

Diffraction patterns of lysozyme were simulated using the Condor package.[40] These were then assembled using EMC and EEMC, using a range of different beam stops and including a range of differently sized sets of diffraction patterns. See Supporting Information for a full description of the orientation recovery.

Acknowledgement

The authors thank the following funding sources: European Union's 7:th Framework Programme and the Swedish Research Council (EGM for a Marie Skłodowska Curie International Career Grant, 2015-00559; CC for project 2013-03940); Royal Society (JLPB for a University Research Fellowship); Engineering & Physical Sciences Research Council (EGM and JLPB, EP/J01835X/1); Swedish Foundation for Strategic Research (CC for an Ingvar Carlsson Award); the Helmholtz Association through the Center for Free-Electron Laser Science at DESY (CC and TE). We would like to acknowledge the use of the University of Oxford Advanced Research Computing (ARC) facility and the Uppsala Multidisciplinary Center for

Advanced Computational Science (UPPMAX, project c2015035) provided by SNIC, in carrying out this work. David van der Spoel and Alexei Abrikossov are thankfully acknowledged for valuable discussions and calculations at an initial stage of this investigation.

Supporting Information Available

The following files are available free of charge.

- si.pdf: Supplementary methods and supplementary figures.
- SI_video1.avi: Video of ubiqitin becoming oriented in 6000 kV cm^{-1}.
- SI_video2.avi: Video of ubiqitin unfolding in 30 000 kV cm^{-1}

References

(1) Russel, D.; Lasker, K.; Phillips, J.; Schneidman-Duhovny, D.; Velazquez-Muriel, J. A.; Sali, A. The structural dynamics of macromolecular processes. *Curr. Op. Cell Biol.* **2009**, *21*, 97–108.

(2) Baldwin, A. J.; Lioe, H.; Hilton, G. R.; Baker, L. A.; Rubinstein, J. L.; Kay, L. E.; Benesch, J. L. P. The Polydispersity of alpha B-Crystallin Is Rationalized by an Interconverting Polyhedral Architecture. *Structure* **2011**, *19*, 1855–1863.

(3) Lanucara, F.; Holman, S. W.; Gray, C. J.; Eyers, C. E. The power of ion mobility-mass spectrometry for structural characterization and the study of conformational dynamics. *Nat. Chem.* **2014**, *6*, 281–294.

(4) Wyttenbach, T.; Pierson, N. A.; Clemmer, D. E.; Bowers, M. T. Ion Mobility Analysis of Molecular Dynamics. *Annu. Rev. Phys. Chem.* **2014**, *65*, 175–196.

(5) Neutze, R.; Wouts, R.; van der Spoel, D.; Weckert, E.; Hajdu, J. Potential for biomolecular imaging with femtosecond X-ray pulses. *Nature* **2000**, *406*, 752–757.

(6) Bogan, M. J.; Benner, W. H.; Boutet, S.; Rohner, U.; Frank, M.; Barty, A.; Seibert, M. M.; Maia, F.; Marchesini, S.; Bajt, S. et al. Single Particle X-ray Diffractive Imaging. *Nano Lett.* **2008**, *8*, 310–316.

(7) Kupitz, C.; Basu, S.; Grotjohann, I.; Fromme, R.; Zatsepin, N. A.; Rendek, K. N.; Hunter, M. S.; Shoeman, R. L.; White, T. A.; Wang, D. et al. Serial time-resolved crystallography of photosystem II using a femtosecond X-ray laser. *Nature* **2014**, *513*, 261–265.

(8) Stagno, J. R.; Liu, Y.; Bhandari, Y. R.; Conrad, C. E.; Panja, S.; Swain, M.; Fan, L.; Nelson, G.; Li, C.; Wendel, D. R. et al. Structures of riboswitch RNA reaction states by mix-and-inject XFEL serial crystallography. *Nature* **2017**, *541*, 242–246.

(9) Colletier, J.-P.; Sawaya, M. R.; Gingery, M.; Rodriguez, J. A.; Cascio, D.; Brewster, A. S.; Michels-Clark, T.; Hice, R. H.; Coquelle, N.; Boutet, S. et al. De novo phasing with X-ray laser reveals mosquito larvicide BinAB structure. *Nature* **2016**, *539*, 43–47.

(10) Seibert, M. M.; Ekeberg, T.; Maia, F. R. N. C.; Svenda, M.; Andreasson, J.; Jonsson, O.; Odic, D.; Iwan, B.; Rocker, A.; Westphal, D. et al. Single mimivirus particles intercepted and imaged with an X-ray laser. *Nature* **2011**, *470*, 78–81.

(11) Ekeberg, T. E.; Svenda, M.; Abergel, C.; Maia, F. R. N. C.; Seltzer, V.; Claverie, J.-M.; Hantke, M.; Joensson, O.; Nettelblad, C.; van der Schot, G. et al. Three-Dimensional Reconstruction of the Giant Mimivirus Particle with an X-Ray Free-Electron Laser. *Phys. Rev. Lett.* **2015**, *114*, 098102.

(12) Chapman, H. N.; Caleman, C.; Timneanu, N. Diffraction before destruction. *Phil. Trans. Royal Soc. B* **2014**, *369*.

(13) Aquila, A.; Barty, A.; Bostedt, C.; Boutet, S.; Carini, G.; dePonte, D.; Drell, P.; Doniach, S.; Downing, K. H.; Earnest, T. et al. The linac coherent light source single particle imaging road map. *Struct. Dyn.* **2015**, *2*, 041701.

(14) Loh, N.-T. D.; Elser, V. Reconstruction algorithm for single-particle diffraction imaging experiments. *Phys. Rev. E Stat. Nonlin. Soft Matt. Phys.* **2009**, *80*, 026705.

(15) Spence, J. C. H.; Schmidt, K.; Wu, J. S.; Hembree, G.; Weierstall, U.; Doak, B.; Fromme, P. Diffraction and imaging from a beam of laser-aligned proteins: Resolution limits. *Acta Crystallogr. Sect. A* **2005**, *61*, 237–245.

(16) Friedrich, B.; Herschbach, D. On the possiblility of orienting rotationally cooled polar-molecules in an electric-field. *Z. Phys. D.* **1991**, *18*, 153–161.

(17) Friedrich, B.; Herschbach, D. Spatial orientation of molecules in strong electric-fields and evidence for pendular states. *Nature* **1991**, *353*, 412–414.

(18) Friedrich, B.; Pullman, D.; Herschbach, D. Alignment and orientation of rotationally cool molecules. *J. Phys. Chem.* **1991**, *95*, 8118–8129.

(19) Rost, J.; Griffin, J.; Freidrich, B.; Herschbach, D. Pendular states and spectra of oriented linear-molecules. *Phys. Rev. Lett.* **1992**, *68*, 1299–1301.

(20) Moore, D.; Oudejans, L.; Miller, R. Pendular state spectroscopy of an asymmetric top: Parallel and perpendicular bands of acetylene-HF. *J. Chem. Phys* **1999**, *110*, 197–208.

(21) Viftrup, S. S.; Kumarappan, V.; Trippel, S.; Stapelfeldt, H.; Hamilton, E.; Seideman, T. Holding and spinning molecules in space. *Phys. Rev. Lett.* **2007**, *99*.

(22) Küpper, J.; Stern, S.; Holmegaard, L.; Filsinger, F.; Rouzee, A.; Rudenko, A.; Johnsson, P.; Martin, A. V.; Adolph, M.; Aquila, A. et al. X-Ray Diffraction from Isolated and Strongly Aligned Gas-Phase Molecules with a Free-Electron Laser. *Phys. Rev. Lett.* **2014**, *112*, 083002.

(23) Shvartsburg, A. A.; Bryskiewicz, T.; Purves, R. W.; Tang, K.; Guevremont, R.; Smith, R. D. Field asymmetric waveform ion mobility spectrometry studies of proteins: Dipole alignment in ion mobility spectrometry? *J. Phys. Chem. B* **2006**, *110*, 21966–21980.

(24) Wilks, A.; Hart, M.; Koehl, A.; Somerville, J.; Boyle, B.; Ruiz-Alonso, D. Characterization of a miniature, ultra-high-field, ion mobility spectrometer. *Int. J. Ion Mobil. Spectrom.* **2012**, *15*, 199–222.

(25) Shvartsburg, A. A.; Smith, R. D. Protein Analyses Using Differential Ion Mobility Microchips with Mass Spectrometry. *Anal. Chem.* **2012**, *84*, 7297–7300.

(26) Bekard, I.; Dunstan, D. E. Electric field induced changes in protein conformation. *Soft Matter* **2014**, *10*, 431–437.

(27) Antoine, R.; Compagnon, I.; Rayane, D.; Broyer, M.; Dugourd, P.; Breaux, G.; Hagemeister, F. C.; Pippen, D.; Hudgins, R. R.; Jarrold, M. F. Electric Susceptibility of Unsolvated Glycine-Based Peptides. *J. Am. Chem. Soc.* **2002**, *124*, 6737–6741.

(28) Bailey, D. S.; Hiskes, J. R.; Riviere, A. C. Electric field ionization probabilities for hydrogen atom. *Nucl. Fusion* **1965**, *5*, 41–46.

(29) Patriksson, A.; Marklund, E.; van der Spoel, D. Protein Structures under Electrospray Conditions. *Biochemistry* **2007**, *46*, 933–945.

(30) Marklund, E. G.; Larsson, D. S. D.; van der Spoel, D.; Patriksson, A.; Caleman, C. Structural stability of electrosprayed proteins: Temperature and hydration effects. *Phys. Chem. Chem. Phys.* **2009**, *11*, 8069.

(31) Brown, L. J.; Toutoungi, D. E.; Devenport, N. A.; Reynolds, J. C.; Kaur-Atwal, G.; Boyle, P.; Creaser, C. S. Miniaturized Ultra High Field Asymmetric Waveform Ion

Mobility Spectrometry Combined with Mass Spectrometry for Peptide Analysis. *Anal. Chem.* **2010**, *82*, 9827–9834.

(32) Horke, D. A.; Chang, Y.-P.; Długołęcki, K.; Küpper, J. Separating *Para* and *Ortho* Water. *Angew. Chem. Int. Ed.* **2014**, *53*, 11965–11968.

(33) van de Meerakker, S. Y. T.; Bethlem, H. L.; Vanhaecke, N.; Meijer, G. Manipulation and Control of Molecular Beams. *Chem. Rev.* **2012**, *112*, 4828–4878.

(34) Hekstra, D. R.; White, K. I.; Socolichclose, M. A.; Henning, R. W.; Šrajer, V.; Ranganathan, R. Electric-field-stimulated protein mechanics. *Nature* **2016**, *540*, 400–405.

(35) Friedrich, B.; Herschbach, D. Manipulating molecules via combined static and laser fields. *J. Phys. Chem. A* **1999**, *103*, 10280–10288.

(36) Friedrich, B.; Herschbach, D. Enhanced orientation of polar molecules by combined electrostatic and nonresonant induced dipole forces. *J. Chem. Phys.* **1999**, *111*, 6157–6160.

(37) Kaltashov, I.; Mohimen, A. Estimates of protein surface areas in solution by electrospray ionization mass spectrometry. *Anal. Chem.* **2005**, *77*, 5370–5379.

(38) Li, J.; Santambrogio, C.; Brocca, S.; Rossetti, G.; Carloni, P.; Grandori, R. Conformational effects in protein electrospray-ionization mass spectrometry. *Mass Spectrom. Rev.* **2016**, *35*, 111–122.

(39) Hess, B.; Kutzner, C.; van der Spoel, D.; Lindahl, E. GROMACS 4: Algorithms for highly efficient, load-balanced, and scalable molecular simulation. *J. Chem. Theory Comput.* **2008**, *4*, 435–447.

(40) Hantke, M. F.; Ekeberg, T.; Maia, F. R. N. C. Condor: A simulation tool for flash X-ray imaging. *J. App. Cryst.* **2016**, *49*, 1356–1362.